

Geochemical and sedimentological analyses on the Romanian *Sphagnum* peat bog Tăul fără fund

Tamás Zsolt Vári¹, Pál Sümegei^{1,2}

¹Department of Geology and Palaeontology, University of Szeged, Szeged, Hungary

²INTERACT AMS Laboratory Nuclear Research Centre, Debrecen, Hungary

SUMMARY

This study focuses on palaeoenvironmental changes in the Bottomless Lake (Tăul fără fund) *Sphagnum* peat bog situated near Băgău in Romania. The central research question was how the lake has changed over time, and how environmental factors and human activities have influenced the changes. By employing previous loss-on-ignition and radiocarbon analyses in addition to new radiocarbon, grain size, magnetic susceptibility and geochemical analyses, a more precise reconstruction of the bog's regeneration and erosion phases was achieved. A multi-proxy analysis of the core sequence provided crucial insights regarding the interconnections between various elements. Notably, plant-derived elements (Na, K) exhibited correlations with organic matter, and carbonate elements (Ca, Mg) with carbonate content; while Fe and magnetic susceptibility displayed changes in relation to inorganic matter content. Remarkably, the findings reflected the global 8200 cal BP and 4200 cal BP events, along with their environmental effects, within the Transylvanian Basin. There was mediaeval lakebed cleaning around 500–300 cal BP, during which the deeper of two water layers was contaminated with more recent materials. The shallower water layer is connected with the modern water circulation, which reduces the apparent age of peat samples taken from its immediate vicinity.

KEY WORDS: AMS radiocarbon dating, geochemistry, Holocene, Quaternary, Romania, sedimentology

INTRODUCTION

Peatlands in Hungary and Romania (Transylvania) have attracted scientific exploration led by the Hungarian Academy of Sciences Institute of Archaeology and the Hungarian Peat Research Society (Magyar Tőzegkutató Társaság), a research group established at the University of Szeged. The principal objective of these endeavours was to decipher the intricate processes that shaped the formation and transformation of peat areas and layers during the final stages of the Quaternary period. Within these peatlands and wetlands lies a wealth of historical environmental and palaeoclimatic information crucial to understanding the culmination of the Quaternary period (Sümegei *et al.* 1999, Sümegei 2001, Joosten & Clarke 2002, Rydin & Jeglum 2006, Tanțău *et al.* 2014, Vári *et al.* 2023).

Selection of the precise sampling location was based on the foundational contributions of Emil Pop (Pop 1932, 1960) and other prior analyses (Vári *et al.* 2020a, 2020b; Benkő *et al.* 2022), which also provided a sturdy platform for further investigations. For geochemical aspects of the peat sequence, water-soluble element content analyses were selected. To comprehend the relationship between sediment size and the processes of erosion and peat formation,

grain size analyses were chosen. Additionally, the correlation between human influences and the magnetic properties of the sediments and peat were studied.

In a comprehensive exploration of the peatland's history spanning approximately 8600 years before present (BP), this new study seeks answers to the following pivotal questions:

- How has the peat bog evolved over time, and what are the key phases of regeneration and erosion that have shaped its present state?
- Which sedimentological and geochemical components are connected to each other?
- What role have natural environmental factors, such as climate variations and human activities, played in driving the observed changes in the bog's palaeoenvironment?
- Are different significant global or regional events like the 8200 and 4200 cal BP events recognisable in the sequence?

Although some of these questions were partially addressed or to some degree answered in previous studies (Vári *et al.* 2020a, 2020b; Benkő *et al.* 2022), this article aims to provide a more comprehensive analysis and final answers. By amalgamating historical and previous data with new multi-proxy



analyses, our study reconstructs the peat bog's evolutionary phases and sheds light on the intricate relationship between natural processes and human influence. The evidence of significant global events and effects of mediaeval lakebed cleaning underscores the importance of our findings in the broader context of regional and global environmental history. Ultimately, this study contributes to our understanding of palaeoenvironmental dynamics whilst highlighting the significance of peat bogs as invaluable windows into the past.

METHODS

Study area

Located in the central Transylvania region of Romania (Figure 1), the Bottomless Lake (Tăul fără fund) lies near the village of Băgău (Magyarbagó) within the Lopadei Hills, which are part of the Târnava Mică Hills. The lake is situated between the Mureş River and the Târnava Mică River. The region has an annual mean temperature around 9–10 °C and annual mean precipitation around 500 mm (Mărculeţ & Mărculeţ 2016). The area is covered by Quaternary fluvial and alluvial sediments and the bedrock consists of Miocene marl and dacite tuff (Stefanescu *et al.* 2006). Various rock-influenced soils (rendzina types) and water-influenced (hydromorphic) soils have developed both in the immediate vicinity of the Bottomless Lake and in the broader region of the Lopadei Hills. In the Lopadei Hills, water-influenced acid peat soils, classified as Histosols, can be found. Forested areas exhibit brown forest soils (Cambisols), while grazing, ploughing and growing crops have led to the development of Anthrosols. The various versions and transitions of these three soil

types can be observed within - and characterise - the study area, whereas the broader region exhibits a much more diverse soil cover (Vári 2021).

Sedimentological and geochemical analysis

A core was collected (Figure 1d) using a Russian peat corer (5 cm in diameter) with an overlapping method (Aaby & Digerfeldt 1986, De Vleeschouwer *et al.* 2010) from the centre of the bog (Vári *et al.* 2020a, 2020b). The sediment sections were wrapped in clingfilm then aluminium foil, and properly stored under dark and cold conditions (4 °C). The depth of the coring was 860 cm, which included two water layers (Vári *et al.* 2020a, 2020b; Benkő *et al.* 2022). Munsell colour (Munsell Color Company 1954) and Troels-Smith classification (Troels-Smith 1955, Vári *et al.* 2020a, 2020b) descriptions were captured in the field.

The loss on ignition (LOI; Dean 1974) data were obtained from previous analyses of material from the same core (Vári *et al.* 2020a, 2020b).

The grain size data were collected at depth intervals of 4 cm and the measurements followed the method described by Sümeği *et al.* (2015). The measurements covered 42 different grain size categories ranging from 0.1 µm to 500 µm, and were obtained using laser diffraction with the OMEC 'Easysizer20' laser particle sizer. The Easysizer20 simplifies the process by automatically performing all measurement steps once the initial parameters are set, ensuring both user-friendly operation and precise outcomes.

Magnetic susceptibility analyses were conducted on bulk samples (Oldfield *et al.* 1978, Dearing 1994). Samples were taken at 4 cm intervals. All samples were weighed then crushed in a glass mortar prior to measurement. Then the samples were placed in plastic boxes and dried in an oven at 40 °C for

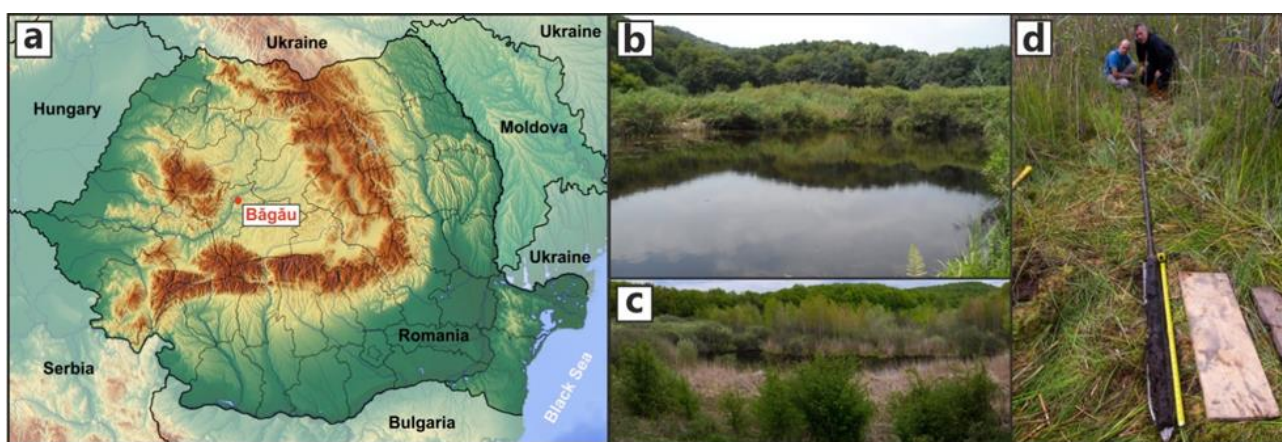


Figure 1. (a) Map of Romania (Vári *et al.* 2020a) showing the location of Băgău. (b, c) Open-water surface of the lake and the nearby vegetation. (d) The coring location with a fresh core still inside the Russian corer.

24 hours. Subsequently, magnetic susceptibilities were measured at a frequency of 2 kHz using an MS2 Bartington magnetic susceptibility meter with an MS2E high-resolution sensor (Dearing 1994). Each sample was measured three times, and the average value of magnetic susceptibility was computed and reported. The samples were used later for other analyses, since this measuring method does not destroy them.

The content of the water-soluble elements calcium (Ca), magnesium (Mg), sodium (Na), potassium (K) and iron (Fe) in the samples was determined using Dr Péter Dániel's sequential extraction geochemical analysis method with a 4 cm sample interval (Dániel *et al.* 1996, Dániel 2004).

Radiocarbon analysis

The preparation of samples for AMS dating and the actual steps of the measurement followed the methods of Hertelendi *et al.* (1989, 1995) and Molnár *et al.* (2013a, 2013b). All of the samples dated were bulk peat (unprocessed organic matter). 1 cm thick samples were put into small transparent sample bags which were labelled with name (“MB” for Magyarbagó) and depth in cm. These samples were stored in dark and cool (4 °C) conditions until they were measured at the DirectAMS Laboratory in Seattle, USA and at the Hertelendi Laboratory of Environmental Studies (HEKAL) in the Institute for Nuclear Research of The Hungarian Academy of Sciences in Debrecen, Hungary (Molnár *et al.* 2013a, 2013b; Rinyu *et al.* 2015, Janovics *et al.* 2018). Samples were treated in the same way in both laboratories, using the standard acid-base-acid (ABA) method following standard protocols (Molnár *et al.* 2013a, 2013b). In this method, the sample is treated with a sequence of 1N HCl, distilled water, 1M NaOH, distilled water, then 1N HCl. After the final acid wash, the sample is washed again with distilled water to neutral pH (4–5) and then freeze-dried. The sample is then ready for combustion. Approximately 5 mg of dry peat was combusted with 300 mg MnO₂ in a vacuum-evacuated (<10–5 mbar) sealed glass test tube at 550 °C for 12 hr. A dedicated vacuum line was used for the purification of liberated CO₂ gas from the H₂O and other gas phase contaminants. The carbon yield was measured volumetrically in the vacuum line (Janovics *et al.* 2018). All of the samples gave at least 40 % m/m C yield and 2 mg of C. A sealed tube graphitisation method was then used to convert the pure CO₂ to graphite (Hammer *et al.* 2001). During the AMS measurement, the ¹⁴C/¹²C and ¹³C/¹²C isotopic quotients were measured simultaneously for the ¹³C correction (Synal *et al.* 2007, Molnár *et al.* 2013a,

2013b). For ¹⁴C data evaluation, “Bats” data reduction software was used (Wacker *et al.* 2010).

Radiocarbon ages were converted to calendar ages using OxCal 4.4 with the Intcal20 calibration curve (Bronk Ramsey 2009, Reimer *et al.* 2020). The Bayesian age-depth modelling (Bronk Ramsey 2009) was performed with RBacon 2.5.8, with two hiatus intervals (90–100 and 406–448 cm) and a 2 cm section interval in RStudio 2022.02.1 Build 461, with the IntCal20 calibration curve (Blaauw & Christen 2011, Reimer *et al.* 2020).

Statistical analysis

Statistical analysis was performed using PAST 3 palaeontological data analysis software (Hammer *et al.* 2001). Principal Component Analysis (PCA) was used to identify the main factors that control elemental distribution in the core section. Before analysis, all data were converted to Z-scores calculated as $(X_i - X_{avg})/X_{std}$, where X_i is the variable and X_{avg} and X_{std} are the series average and standard deviation, respectively, of the variable X_i (Davis 1986, Eriksson *et al.* 1999).

RESULTS

Radiocarbon analysis

Sample DeA-20923 (44 cm) produced an impossible age of -1461 BP ± 25 uncal BP, which is likely to have resulted from the modern era pollution and contamination that is also evidenced by its F¹⁴C value of 1.1994 ± 0.0037 (Table 1). Although the HEKAL laboratory estimated the calibrated age of DeA-20923 at 1959–1981 AD, this sample cannot be taken into Bacon modelling or OxCal calibration because it produces an unacceptable date even if we apply BombCal21 (Hua *et al.* 2021) instead of IntCal20 (Blaauw & Christen 2011, Reimer *et al.* 2020).

Sample DeA-20924 (88 cm) is also excluded from the modelling because the results suggest that the water layer (90–100 cm) has been in contact with surface water (e.g., recent rainfall, inflows) which contaminated the peat in the vicinity of the water. Based on the F¹⁴C value (1.0082 ± 0.0032), this contamination happened around 1900–1960 AD (unmodelled, calibrated, 99.7 %, 88 cm). Comparing the multi-proxy results between the two water layers (Figure 2) and the unmodelled radiocarbon ages (Table 1), there is evidence for an anthropogenic intervention (digging) at 176–230 cm, which disturbed the sequence and the Bottomless Lake. At 255 cm (D-AMS 17150), the F¹⁴C value is around the expected value (0.7332 ± 0.0051) and is unaffected by the consequences of the digging.

Table 1. Results of ^{14}C AMS analysis of the core: unmodelled uncalibrated and calibrated BP ages.

Laboratory code	Depth (cm)	BP	$F^{14}\text{C} + 1\sigma$	Unmodelled cal BP (68.3%)	Unmodelled cal BP (95.4%)	Unmodelled cal BP (99.7%)	Unmodelled cal BP	
							$\mu + \sigma$	median
DeA-20923	44	-1461 ± 25	1.1994 ± 0.0037	-	-	-	-	-
D-AMS 17148	60	284 ± 36	0.9653 ± 0.0043	430–290	460–150	500–20	360 ± 70	380
DeA-20924	88	-66 ± 26	1.0082 ± 0.0032	20–(-10)	30–(-10)	50–(-10)	10 ± 10	10
D-AMS 032147	180	315 ± 24	0.9616 ± 0.0029	430–310	460–300	480–290	380 ± 40	390
D-AMS 17149	185	333 ± 21	0.9594 ± 0.0025	450–310	470–310	490–300	390 ± 40	380
D-AMS 032146	186	343 ± 23	0.9582 ± 0.0028	460–310	480–310	500–300	390 ± 50	390
D-AMS 20195	190	393 ± 42	0.9522 ± 0.0050	510–330	520–310	530–300	430 ± 60	450
DeA-20925	202	427 ± 27	0.9483 ± 0.0031	510–480	530–330	540–320	490 ± 40	500
D-AMS 17150	255	2286 ± 29	0.7523 ± 0.0027	2350–2180	2360–2150	2360–2150	2280 ± 60	2320
D-AMS 20196	280	2493 ± 56	0.7332 ± 0.0051	2720–2490	2740–2360	2760–2350	2570 ± 100	2570
DeA-20926	302	2962 ± 74	0.6917 ± 0.0064	3230–3000	3360–2930	3400–2840	3130 ± 110	3130
D-AMS 17151	360	3069 ± 32	0.6825 ± 0.0027	3350–3230	3370–3170	3400–3140	3280 ± 50	3280
D-AMS 17152	460	380 ± 20	0.9538 ± 0.0024	493–335	499–327	505–316	431 ± 58	459
D-AMS 17153	559	4144 ± 24	0.5970 ± 0.0018	4820–4580	4830–4570	4830–4520	4690 ± 70	4690
D-AMS 16726	658	5665 ± 49	0.4940 ± 0.0030	6500–6350	6600–6310	6640–6290	6450 ± 70	6450
DeA-20927	732	6058 ± 37	0.4705 ± 0.0021	6960–6800	7150–6790	7160–6740	6910 ± 70	6910
DeA-20928	780	6207 ± 36	0.4619 ± 0.0020	7170–7010	7250–6990	7260–6950	7100 ± 70	7090
D-AMS 16725	800	6349 ± 67	0.4537 ± 0.0038	7420–7160	7430–7080	7440–6990	7270 ± 80	7270
D-AMS 20197	820	6372 ± 50	0.4524 ± 0.0028	7420–7170	7430–7160	7430–7160	7300 ± 70	7300
D-AMS 16724	829	6443 ± 38	0.4484 ± 0.0021	7430–7320	7430–7270	7470–7170	7360 ± 40	7360
D-AMS 20198	846	7709 ± 44	0.3830 ± 0.0021	8540–8430	8590–8410	8610–7380	8490 ± 50	8490

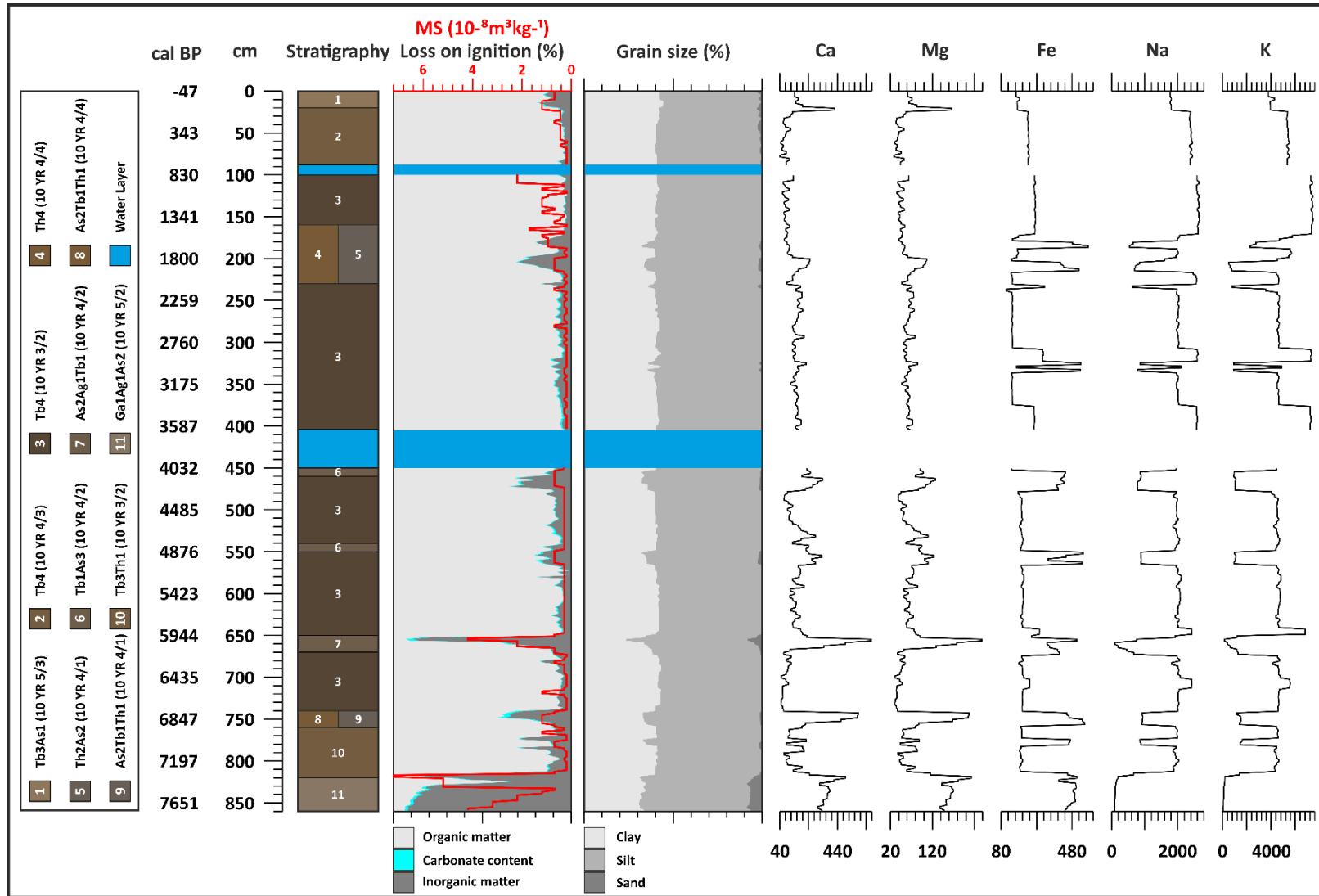


Figure 2. Calibrated ages (modelled using Model (b) in Figure 3) every 50 cm, depth in cm, stratigraphy (Vári *et al.* 2020a), loss on ignition (LOI) results (%), magnetic susceptibility (MS) results (10⁻⁸ m³ kg⁻¹), grain size results (%) and geochemistry (ppm). The blue bands indicate water layers.



Sample D-AMS 17152 (460 cm) was also excluded from the modelling, since it produced a surprising age of 380 ± 20 uncal BP and a high $F^{14}C$ value of 0.9538 ± 0.0024 . To cause this, the water layer at 448–406 cm must have been in contact with either younger materials or, more probably, with a water circulation system connected to the surface, around 1440–1640 AD (unmodelled, calibrated, 99.7 %, 460 cm). This contact contaminated peat in the vicinity of the water layer and the peat sequence, hence the younger age. Based on the similarities in uncalibrated age, calibrated age and $F^{14}C$ values (Table 1), we link this event to the presumed anthropogenic excavation of the lake to create a larger open-water surface for secure water supply (Benkő *et al.* 2022).

Corrections were made to the previous depths as they were found to be inaccurate, and this adjustment is supported by the $F^{14}C$ values obtained from samples D-AMS 016724, 016725, 016726, 032146, 032147, 017149, 017150, 017151, 017153, 01715, 020195, 020197 and 020198 (Benkő *et al.* 2022). Additionally, the original percent modern carbon (pMC) values were converted to Fraction Modern ($F^{14}C$) values based on the laboratory reports (Table 1, Figure 3.).

Due to the contaminations, two models were made (Figure 3). Model (a) was made without the samples at 44, 88 and 460 cm; and Model (b) without the samples at 44, 88, 180, 185, 186, 190, 202 and 460 cm. This means the anthropogenic effect between 160 and 230 cm, which caused younger ages, is left out in Model (b). Both models (Figure 3, Table 2) give an approximately thousand-year-younger beginning compared to Benkő *et al.* 2022 for the sediment accumulation at the bottom of the core, and modelled cal BP median ages that are close to each other during most of the sequence. Model (b) is suggested for examining peat growth and sediment deposition, because it excludes the main anthropogenic effect and removes the effect of modern contamination on the age-depth model.

To gain a visual understanding of the data, calibrated modelled dates from Model (b) (Table 2) were assigned to every 50 cm increment in Figure 2. The deposition of sediment began with the slow accumulation of inorganic sediment, but accelerated once it started to accumulate organic matter, which had a uniform and rapid accumulation rate of around 1 mm year⁻¹ (Figure 3b). This means that the environment was suitable for the accumulation of *Sphagnum* peat, which was interrupted for only a short time by minor weathering, erosion and anthropogenic effects. Modelled BP dates and ages used in the text and Figures are calibrated median

ages from Model (b) (Table 2).

The radiocarbon sample DeA-20925 (202 cm) indicates dredging of the lakebed. It is likely that this human intervention occurred during the time window 530–330 cal BP (1420–1620 AD).

Sedimentological analysis

By analysing how the magnetic properties of the sediment change over time, we can gain insights into the past intensity of weathering. Weathering, in turn, influences the amount of ferromagnetic minerals deposited in the sediment. Interestingly, the magnetic susceptibility (MS) values are very low throughout the profile, and these variations correlate with geochemical data (probably Fe content) only in the lower section. It is likely that the low MS is due to waterlogging, which has transformed the ferromagnetic minerals (Sandgren & Snowball 2002). Overall, the MS analyses (Figure 2) exhibit a correlation with fluctuations in carbonate and inorganic material content, as well as with the concentrations of Ca, Mg and Fe. This indicates that the MS values oscillate between peaks caused by erosion events and low values during periods of peat regeneration. Notably, the MS values during phases of peat formation are extremely low. The peak values during soil erosion phases are low compared to other peat bogs (Tapody *et al.* 2018, 2021; Magiera *et al.* 2021), with values of $0.5\text{--}7 \times 10^{-8} \text{ m}^{-3} \text{ kg}^{-1}$. The highest and second highest values are in the lower part of the sequence between 832 and 820 cm. Magnetic susceptibility increases abruptly after the mediaeval anthropogenic interruption (Benkő *et al.* 2022), from around 230 cm up to 100 cm, after which it drops before increasing again towards the surface.

Sediments with grain sizes typical of clay and silt characterise peat accumulation (Figure 2) but silt-sized sediments, together with the sand fraction, also reflect weathering and erosion events. The changes in grain size fractions (Clay, Silt, Sand) are consistent with the processes of peat formation and deposition of inorganic sediments throughout the core sequence. On average, the core can be characterised as 39.45 % clay, 59.52 % silt and 1.05 % sand. The following intervals display increased Silt and Sand suggesting erosion events: 784–774 cm, 756–742 cm, 672–650 cm, 564–550 cm, 476–454 cm, 334–332 cm, 326–324 cm, 234–232 cm, 216–200 cm, 190–180 cm and 74–0 cm. These erosion intervals correlate with the MS and geochemical results, as well as with the major inorganic matter content peaks.

The Polish lake bottom classification system (Figure 4) (Kabała *et al.* 2019, Łachacz & Nitkiewicz 2021, Vári *et al.* 2023), which is based on data from LOI analysis (Figure 2) (Vári *et al.* 2020a, 2020b),

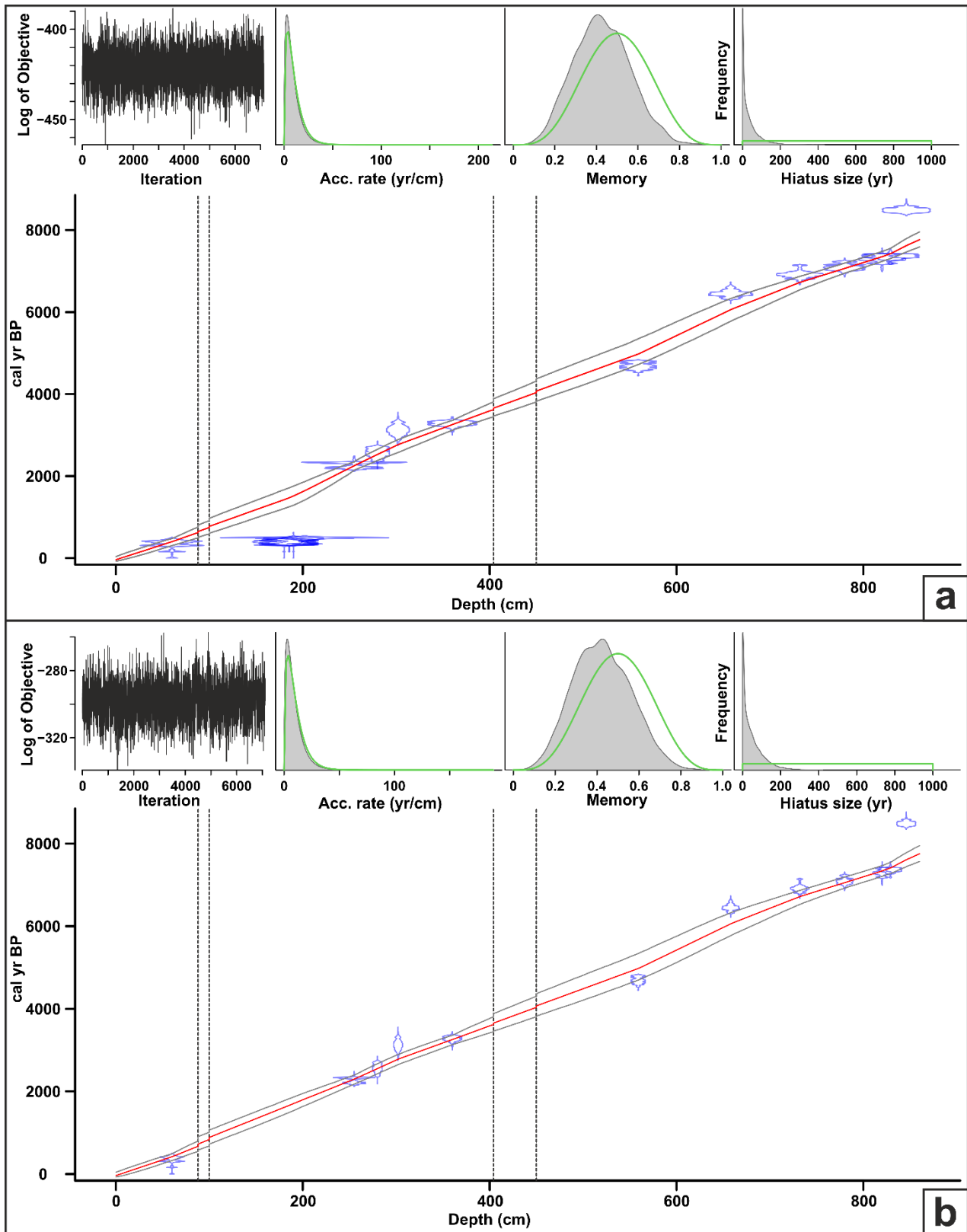


Figure 3. Results of the age-depth modelling. Model (a) is without the samples at 44, 88 and 460 cm. Model (b) is calculated without the samples at 44, 88, 180, 185, 186, 190, 202 and 460 cm. The water layers (90–100 cm and 406–448 cm) are set as hiatus depths. Settings for both models: acc.shape: 1.5; acc.mean: 10; mem.strength: 10; mem.mean: 0.5; hiatus max: 1000; 432 × 2 cm sections.

Table 2. Age-depth modelling results; modelled calibrated BP ages for every 20 cm with Models (a) and (b).

Depth (cm)	Modelled cal BP (a)			Modelled cal BP (b)		
	(95 %)	median	mean	(95 %)	median	mean
0	-72 – 35	-49	-40	-72 – 42	-47	-38
20	32 – 196	104	107	39 – 202	112	114
40	163 – 344	254	254	177 – 354	267	266
60	303 – 478	406	401	324 – 491	419	419
80	440 – 681	561	561	488 – 717	599	600
100	587 – 912	741	743	676 – 1012	830	833
120	753 – 1150	932	937	901 – 1244	1067	1069
140	905 – 1322	1095	1100	1075 – 1422	1251	1250
160	1061 – 1494	1260	1263	1255 – 1602	1433	1432
180	1209 – 1667	1426	1424	1439 – 1778	1614	1613
200	1395 – 1848	1628	1622	1637 – 1950	1800	1798
220	1644 – 2037	1853	1850	1830 – 2111	1981	1977
240	1917 – 2225	2083	2080	2027 – 2274	2167	2161
260	2190 – 2422	2311	2308	2224 – 2451	2353	2348
280	2381 – 2655	2532	2529	2428 – 2671	2554	2553
300	2558 – 2871	2754	2746	2627 – 2875	2760	2759
320	2742 – 3046	2925	2919	2802 – 3047	2930	2929
340	2931 – 3206	3091	3087	2964 – 3209	3093	3092
360	3119 – 3358	3258	3256	3131 – 3358	3257	3255
380	3268 – 3567	3423	3423	3273 – 3570	3421	3421
400	3419 – 3772	3587	3590	3417 – 3768	3586	3587
420	3579 – 4034	3778	3788	3577 – 4028	3775	3786
440	3732 – 4219	3938	3955	3732 – 4215	3940	3952
460	3906 – 4462	4131	4157	3899 – 4456	4133	4154
480	4062 – 4641	4286	4323	4054 – 4635	4293	4320
500	4222 – 4820	4442	4488	4208 – 4813	4455	4485
520	4387 – 4996	4595	4654	4371 – 4992	4618	4651
540	4555 – 5168	4744	4820	4532 – 5163	4790	4818
560	4730 – 5360	4904	4987	4704 – 5351	4961	4986
580	4926 – 5555	5153	5206	4908 – 5557	5174	5204
600	5137 – 5764	5395	5426	5119 – 5758	5401	5423
620	5352 – 5967	5622	5645	5344 – 5965	5625	5642
640	5571 – 6160	5841	5862	5571 – 6161	5840	5861
660	5799 – 6346	6048	6078	5794 – 6344	6047	6077
680	6004 – 6500	6247	6258	6002 – 6498	6242	6256
700	6209 – 6644	6436	6437	6208 – 6643	6432	6435
720	6418 – 6784	6621	6617	6410 – 6785	6615	6612
740	6612 – 6923	6786	6782	6600 – 6923	6779	6775
760	6782 – 7057	6924	6923	6764 – 7060	6917	6915
780	6949 – 7195	7065	7065	6922 – 7193	7055	7055
800	7090 – 7333	7208	7208	7067 – 7325	7197	7197
820	7236 – 7479	7353	7351	7207 – 7468	7341	7339
840	7408 – 7710	7547	7551	7383 – 7701	7539	7540
860	7588 – 7955	7762	7765	7567 – 7949	7753	7753

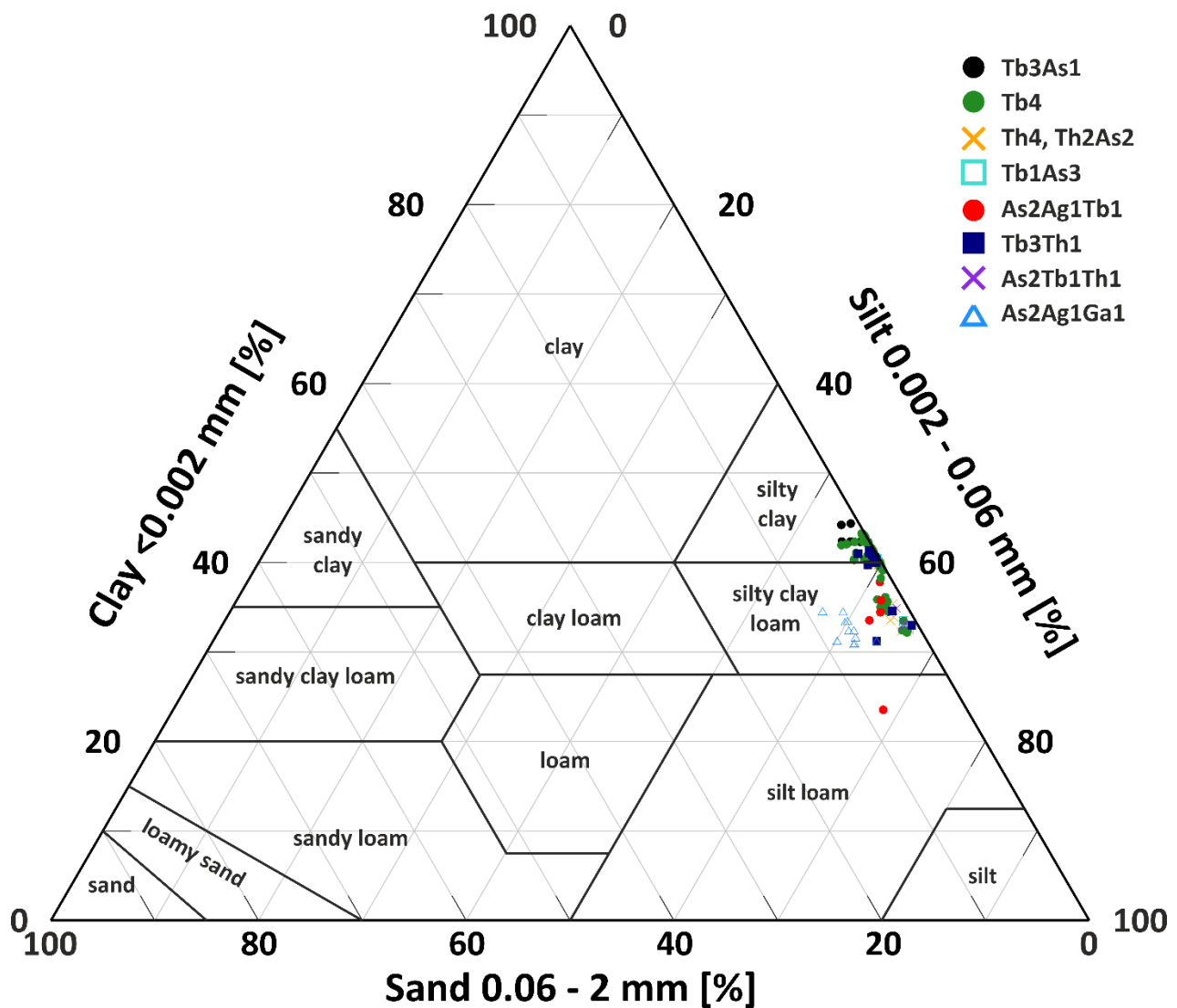


Figure 4. Ternary diagram of clay, silt and sand grain sizes with Troels-Smith sediment types (Troels-Smith 1955), based on the grain size analysis.

and the grain size ternary diagram (Figure 5) were used to differentiate the phases and provide a clearer understanding of the evolution and development of the core sequence. With these systems, it is possible to interpret LOI (Vári *et al.* 2020a, 2020b) and grain size data to describe sediment types, especially if paired with the Troels-Smith classification (Troels-Smith 1955).

The core sequence commenced with the deposition of silty clay loam sediment, and the sediments interpreted to result from erosion events were also classified as silty clay loam. As peat began to accumulate and the organic matter content increased, the sediment types transitioned from clay-detrital gyttja to fine detrital gyttja, followed by coarse detrital gyttja and algal gyttja towards the end. The majority of the sequence was classified as algal

gyttja (Figure 4) and silty clay (Figure 5). It is important to note that the term "detrital gyttja" in this context refers to partially or completely decomposed *Sphagnum* peat of clay and silt grain size, mixed with a small amount of inorganic sediment (Kabała *et al.* 2019, Łachacz & Nitkiewicz 2021).

Geochemical analysis

The variations in water-soluble elements (Figure 2) exhibit strong correlations with organic matter content (OM), inorganic matter content (IM), carbonate content (CC), magnetic susceptibility (MS) and grain size (GS). The values of Ca and Mg change together and correlate more closely with IM and CC. They serve as indicators of the mineral quality of groundwater and show elevated values when the bog comes into contact with Ca-Mg rich bedrock (Shotyk

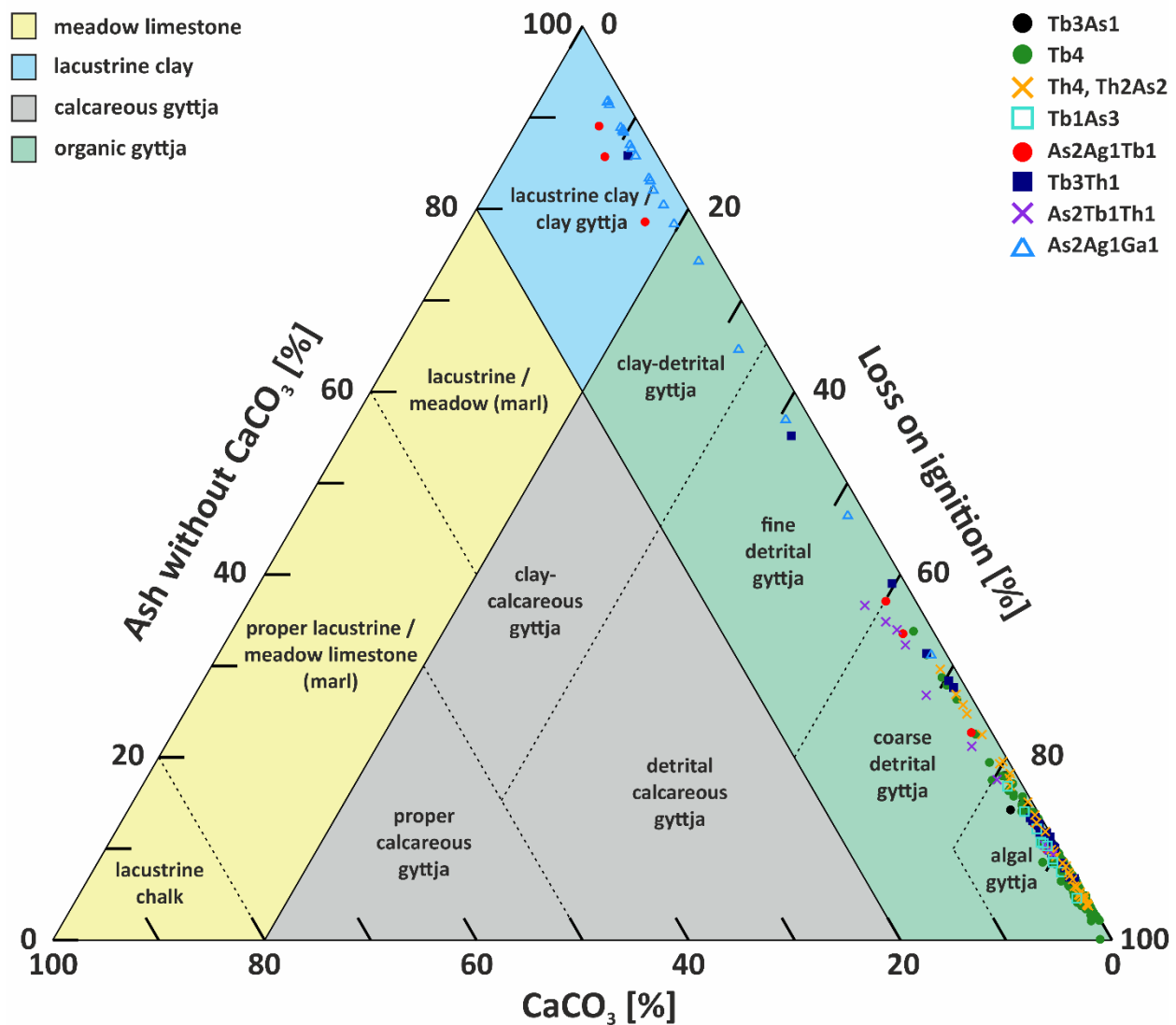


Figure 5. Results of loss on ignition analysis on a ternary plot (organic matter %, inorganic matter %, carbonate content %). Symbols represent the Troels-Smith classification (Troels-Smith 1955), while the background presents the lake-bottom deposit classification system (Kabała *et al.* 2019, Łachacz & Nitkiewicz 2021, Vári *et al.* 2023).

1988), which gets washed in during erosion events. The fluctuations in Ca and Mg align with the movement of IM and CC, suggesting that the origin of carbonates is closely linked to the deposition of allochthonous inorganic sediment. Notably, the highest peaks of both Ca (>600 ppm) and Mg (>200 ppm) are found in the lower part of the sequence (below 650 cm), and they show much lower values in the depth range 650–0 cm. Overall, water-soluble Ca and Mg are the least abundant of the five analysed elements based on their average and maximum ppm values. The average is 168 ppm for Ca and 71 ppm for Mg; the minimum is 45 ppm for Ca and 29 ppm for Mg; and the maximum is 679 ppm for Ca and 239 ppm for Mg.

The changes in Fe content can be attributed to soil erosion and the deposition of inorganic sediments. Fe is a mobile element in specific environments and highly responsive to environmental changes, producing distinct, visible peaks (Shotyk 1988). In our results these high peaks consistently exceed 350–450 ppm, while the average Fe concentration observed is 258 ppm, the minimum is 112 ppm and the maximum is 573 ppm.

The accumulation of Na and K occurs during peat formation, and their concentrations increase with OM content. However, they decrease during erosion events. Following the mediaeval lakebed interruption (Benkő *et al.* 2022), Na and K reach higher values (2600 ppm and 7500 ppm at 172–100 cm), then

decrease after the water layer at 100–90 cm (2400 ppm and 5400 ppm) and continue to gradually decrease towards the surface (1800 ppm and 3800 ppm). The average Na concentration is 1858 ppm, with a minimum value of 99 ppm and a maximum value of 2676 ppm. The average K concentration is 4341 ppm, with a minimum value of 108 ppm and a maximum value of 7509 ppm.

Statistical analysis

Principal component analysis (PCA) was conducted on the complete dataset (LOI, MS, GS and geochemistry) in order to reduce its complexity and identify patterns of variation. The primary objective was to identify two distinct groups: an autochthonous fraction consisting of chemically and biogenically deposited materials correlating with the organic matter content and evidence for peat growth; and an allochthonous fraction representing terrigenous sediment that correlates with IM and CC. Although the first two principal components accounted for the majority of the variance, making them the most informative (Table 3), OM notably exhibited negative loadings in both PC1 and PC2. Thus, additional principal components were necessary to capture components with high loadings and provide valuable information about sedimentological and geochemical relationships and changes:

- PC1 explains the largest proportion of the variance in the dataset (69.36 %) and is characterised by carbonate (CC, Ca, Mg) and inorganic (IM, Fe) elements and MS, Silt and Sand;
- PC2, explaining 10.65 % of the variance, represents elements such as IM, MS, Clay and Sand, while showing lower loadings for CC, Ca, Mg, Na, and K;
- PC3 explains 7.29 % of the variance and reflects the influence of carbonate elements (CC, Ca, Mg), along with Na and K, while having lesser loadings for OM, Clay and Silt.

Cumulatively, PC1–PC3 account for 87.3 % of the variance, which underscores the significance of these principal components in explaining the patterns observed in the dataset. These results reveal that the different events and environments (soil erosion, peat growth) within the peat bog exhibit mixed sedimentological origins (in-situ organic matter accumulation and local weathering alongside human-induced soil erosion and allochthonous dust accumulation), reflecting the influence of a variety of processes. These findings emphasise the intricate nature of palaeoenvironmental changes in the peat bog during the Holocene and highlight the importance of considering multiple processes when interpreting the sedimentological and geochemical characteristics of the sequence.

Table 3. Eigenvalue, % variance and loadings for PC1–PC3. Different typefaces and colours indicate negative (italic, red), positive (regular, black) and highest (bold, green) loadings.

	PC 1	PC 2	PC 3
Eigenvalue	8.32	1.28	0.87
% variance	69.36	10.65	7.29
OM	<i>-0.3091</i>	<i>-0.2981</i>	0.0921
CC	0.2705	0.0484	0.5631
IM	0.3069	0.3040	<i>-0.1156</i>
MS	0.2482	0.3531	<i>-0.2176</i>
Clay	<i>-0.3141</i>	0.2920	0.1122
Silt	0.2249	<i>-0.6132</i>	0.0375
Sand	0.2989	0.2931	<i>-0.2731</i>
Ca	0.2980	0.0186	0.4810
Mg	0.3129	0.0821	0.3709
Na	<i>-0.3076</i>	0.1462	0.2104
K	<i>-0.2915</i>	0.1887	0.1343
Fe	0.2658	<i>-0.2837</i>	<i>-0.3064</i>

DISCUSSION

When analysing the entire peat bog sequence, it becomes evident that the sequence cannot be easily divided into two distinct groups based solely on the origin of elements (allochthonous, autochthonous) using PCA. However, upon examining the LOI, GS, MS and geochemistry results, certain correlations emerge. Ca and Mg exhibit a positive correlation with CC, while Na and K show a correlation with OM. Additionally, Fe and MS, along with silt and sand grain sizes, correlate with IM. These correlations shed light on the relationships between specific elements and the corresponding geochemical characteristics of the peat, providing further insights into the sedimentological and environmental dynamics evidenced by the sequence.

A wetland started to form about 8400–8600 unmodelled cal BP years ago and was initially characterised by a slow accumulation of sediment consisting of mainly inorganic materials, followed by peat accumulation about 8000–8400 unmodelled cal BP years ago. Based on the unmodelled calibrated

ages the Greenlandian-Northgrippian boundary, which coincides with the 8.2 kyr BP event during which global temperatures decreased drastically (Kobashi *et al.* 2007, Cheng *et al.* 2009), correlates with the start of the sequence. The decrease in global temperatures coinciding with a rise in precipitation potentially established the necessary conditions for the formation of the bog. This environmental shift may have affected the cultures in Transylvania, leading to the erosion event that occurred slightly later (818 cm), following the initial accumulation of peat. Linking a single culture to a specific event is not easy, since the Transylvanian Basin has been rich in different cultures, communities and groups during the past 8000 years (Dumitrescu *et al.* 1982, Feurdean *et al.* 2007, Tanțău *et al.* 2009, Grindean *et al.* 2014, Feurdean 2015, Feurdean *et al.* 2015, Tapody *et al.* 2018, Fărcaș *et al.* 2020, Tapody *et al.* 2021, Benkő *et al.* 2022).

In the lower section (860–650 cm, from ca. 7750 to ca. 5950 cal BP) of the core, it is plausible that weathering and erosion significantly influenced the supply of elements and the connection to bedrock was closer during this stage than later. This could explain the elevated levels of Ca and Mg, as well as the possible presence of Na and K originating from inorganic sources. Three major erosion events are tied to this interval, at 784–774 cm, 756–742 cm and 672–650 cm. In this context, the deposition of a considerable amount of clayey silty inorganic sediment (Vári *et al.* 2020a) could be indicative of a larger-scale soil movement or accumulation that effectively sealed off the lake environment from the predominant carbonate-rich bedrock sediments. However, the exact cause of this suggested process, whether it is of natural origin or influenced by human activity, remains uncertain.

Below the lower water layer, the erosion event at 476–454 cm (ca. 4250–4050 cal BP) (Vári *et al.* 2020a, 2020b) aligns well with the aridification event at 4200 BP that signifies the beginning of the Meghalayan era in the Holocene (Staubwasser *et al.* 2003, Cohen *et al.* 2013, Roland *et al.* 2014, Li *et al.* 2018). This alignment is supported by both age-depth models, which place 4200 cal BP in the depth range 460–480 cm. After this drier period, there could have been a wetter period with more precipitation which raised water levels so the peat later formed a floating mat on top of the water surface (Vári *et al.* 2020a, 2020b; Benkő *et al.* 2022).

An additional double erosion event, not mentioned in previous publications (Vári *et al.* 2020a, 2020b; Benkő *et al.* 2022), occurred in the depth range 334–324 cm (2900–3100 modelled cal BP). This event was only discerned following the analysis of grain size and geochemical data.

Concurrently, there was a minor increase in IM and CC, accompanied by a minor increase in Ca and Mg, but Fe exhibited a double peak increase. In contrast, Na and K demonstrated a substantial double peak decrease, while OM experienced a slight decline.

The mediaeval lakebed cleaning (Vári *et al.* 2020a, 2020b; Benkő *et al.* 2022), which occurred around 530–330 cal BP (202 cm) and not during the Roman or Migration period (Vári *et al.* 2020a), is supported by the new results. Ordering of ages for the events between 180 and 255 cm may be misleading due to human intervention, as there is an age difference of nearly 2000 years between 202 cm and 255 cm based on the unmodelled radiocarbon ages (Table 1). The top and bottom dates of the dredging cannot be determined precisely, but three erosion peaks can be recognised at 234–232 cm, 216–200 cm and 190–180 cm, meaning the base of the sedimentary evidence for the human intervention should be around 234–232 cm rather than 218 cm (Benkő *et al.* 2022) and the top is at 180 cm. The other two erosion events, at 216–200 cm and 190–180 cm based on the radiocarbon results, happened around the same time, and were caused by settlers nearby.

Focusing particularly on Fe, Na and K, the geochemical analysis provides no direct evidence of anthropogenic influence on the lake sediment between the depths of 178 cm and 24 cm. However, the MS values display increasing peaks leading up to the water layer (100–90 cm). LOI and grain size results, along with Ca and Mg concentrations, show minor fluctuations up until the water layer (100–90 cm). This water layer is evidently connected to the surface water system, as indicated by the modern age determined from the sample taken at 88 cm. The sample at 44 cm also exhibits a modern age, suggesting that the influence of the recent water system extends downward through the peat layer to approximately 50 cm depth. Fe, Na and K demonstrate a decrease between depths of 24–0 cm, whereas Ca and Mg concentrations exhibit a peak, accompanied by increases in MS and IM.

Overall, the analyses revealed notable correlations between specific elements and their associated parameters, such as Ca and Mg with CC, Na and K with OM, and Fe and sand fraction with IM. Silt (around 60 %) and Clay (around 40 %) dominate the sequence; the grain sizes are classified as silty clay, silty clay loam or silt loam (gyttja) with high (about 85 %) OM. Increased Sand is a sign of an erosion event. The identification of correlations between the elements further enhances our understanding of sedimentological and environmental dynamics within the peat sequence, since correlations between elements can reveal their

source. Thus, the data can be used to reconstruct past environmental conditions; changes in correlations throughout the sequence can track changes in the environment over time; and correlations between certain elements can highlight human influence on the environment.

The research conducted in this area suggests its potential vulnerability to both the 8200 BP and the 4200 BP events. These events hold particular significance in the context of understanding how cultures responded to the altered environment during those time periods. Additionally, it is important to note that the two water layers have encountered younger materials, resulting in contamination in their immediate vicinities. The results also point to significant human-induced interventions in the mediaeval period, as evidenced by the erosion peaks and sediment characteristics observed during that time frame. The alignment of these findings with historical records supports the notion that human activities, such as lakebed cleaning (dredging), have left discernible imprints on the peat bog sequence.

The study's implications extend beyond the boundary of the peat bog itself. The evidence of possible effects of significant global events within the local context emphasises the interconnectedness of regional and global environmental dynamics. Furthermore, the reconstruction of the peatland's evolution serves as a testament to the invaluable role of peatlands as archives of Earth's environmental history, reflecting the intricate interplay of natural processes and human actions like drainage, dredging and fires over time, which can disrupt the delicate balance of a peatland so as to impact its ability to store carbon and thrive.

The multidisciplinary approach employed here serves as a valuable framework for future research on similar lake and peat bog systems, providing insights into their formation, evolution and historical significance. A promising future direction for research would involve conducting pollen analyses to examine alterations in the surrounding vegetation at both local and regional scales. Obtaining these data could further enrich our understanding by enabling a comprehensive study encompassing botanical and geoarchaeological aspects.

ACKNOWLEDGEMENTS

The research was supported by OTKA grant K-112318 (An Environmental History of the Carpathian Basin in the Middle Ages); and was carried out within the framework of University of Szeged, Institute of Geography and Earth Sciences, Long Environmental Changes Research Team.

AUTHOR CONTRIBUTIONS

TZV: conceptualisation, data collection and contribution, performing the analyses, writing original draft, review and editing of subsequent versions. PS: conceptualisation, data collection and contribution, acquisition of funding.

REFERENCES

- Aaby, B., Digerfeldt, G. (1986) Sampling techniques for lakes and mires. In: Berglund, B.E. (ed.) *Handbook of Holocene Palaeoecology and Palaeohydrology*, John Wiley & Sons, Chichester, UK, 181–194.
- Benkő, E., Silye, L., Tóth, A., Pál, I., Frink, J.P., Jakab, G. (2022) Emerging mediaeval heritage: Environmental history research at Băgău (c. Alba, Romania) and the Bottomless Lake (Tăul fără fund). *Acta Archaeologica Academiae Scientiarum Hungaricae*, 73(2), 191–203.
- Blaauw, M., Christen, J.A. (2011) Flexible paleoclimate age-depth models using an autoregressive gamma process. *Bayesian Analysis*, 6(3) 457–474.
- Bronk Ramsey, C. (2009) Bayesian analysis of radiocarbon dates. *Radiocarbon*, 51(1), 337–360.
- Cheng, H., Fleitmann, D., Edwards, R., Wang, X., Cruz, F., Auler, A., Mangin, A., Wang, Y., Kong, X., Burns, S., Matter, A. (2009) Timing and structure of the 8.2 kyr B.P. event inferred from 18O records of stalagmites from China, Oman, and Brazil. *Geology*, 37, 1007–1010.
- Cohen, K.M., Finney, S.C., Gibbard, P.L., Fan, J.-X. (2013) The ICS International Chronostratigraphic Chart. *Episodes*, 36, 199–204.
- Dániel, P. (2004) Results of the geochemical analysis of the samples from Bátorliget II profile. In: Sümeği, P., Gulyás, S. (eds.) *The Geohistory of Bátorliget Marshland*, Archaeolingua Press, Budapest, 95–128.
- Dániel, P., Kovács, B., Győri, Z., Sümeği, P.A. (1996) Combined sequential extraction method for analysis of ions bounded to mineral component. *Abstracts of the 4th Soil and Sediment Contaminant Analysis Workshop*, Lausanne, Switzerland, page 396.
- Davis, J.C. (1986) *Statistics and Data Analysis in Geology*. John Wiley & Sons Inc., New York, 656 pp.
- Dean, W.E. (1974) Determination of carbonate and organic matter in calcareous sediments and sedimentary rocks by loss on ignition; comparison with other methods. *Journal of Sedimentary*

- Petrology*, 44, 242–248.
- Dearing, J.A. (1994) *Environmental Magnetic Susceptibility: Using the Bartington MS2 System*. Chi Publishing, Kenilworth, UK, 104 pp.
- De Vleeschouwer, F., Chambers, F., Swindles, G. (2010) Coring and sub-sampling of peatlands for palaeoenvironmental research. *Mires and Peat*, 7, 01, 10 pp.
- Dumitrescu, V., Bolomey, A., Mogoşanu, F. (1982) The prehistory of Romania from the earliest times to 1000 B.C. In: Boardman, J., Edwards, I.E.S., Hammond, N.G.L., Sollberger, E. (eds.) *The Prehistory of the Balkans and the Middle East and the Aegean World, Tenth to Eight Centuries B.C.*, The Cambridge Ancient History Part 1, Cambridge University Press, Cambridge, UK, 1–74.
- Eriksson, L., Johansson, E., Kettaneh-Wold, N., Wold, S. (1999) Introduction to Multi- and Megavariate Data Analysis Using Projection Methods (PCA & PLS). Umetrics AB, Umeå, Sweden, 490 pp.
- Fărcaş, S., Ursu, T.M., Pop, V.V., Tanţău, I., Roman, A. (2020) Considerations on the age of the “glimee” in Transylvania. *Contributii Botanice*, 55, 109–118.
- Feurdean, A. (2015) Vegetation, climate and fire: new insight from palaeoecological records from the Romania. In: Mindrescu, M. (ed.) *Late Pleistocene and Holocene Climatic Variability in the Carpathian-Balkan Region: Abstracts Volume*, GEOREVIEW: Scientific Annals of Stefan cel Mare University of Suceava, Geography Series, 24(2), 37–38.
- Feurdean, A., Mosbrugger, V., Onac, B.P., Polyak, V., Veres, D. (2007) Younger Dryas to mid-Holocene environmental history of the lowlands of NW Transylvania, Romania. *Quaternary Research*, 68(3), 364–378.
- Feurdean, A., Galka, M., Kuske, E., Tanţău, I., Lamentowicz, M., Florescu, G., Liakka, J., Hutchinson, S.M., Mulch, A., Hickler, T. (2015) Last millennium hydro-climate variability in Central-Eastern Europe (northern Carpathians, Romania). *The Holocene*, 25(7), 1179–1192.
- Grindean, R., Tanţău, I., Fărcaş, S., Panait, A. (2014) Middle to Late Holocene vegetation shifts in the NW Transylvanian lowlands (Romania). *Studia UBB Geologia*, 59(1), 29–37.
- Hammer, O., Harper, D.A.T., Ryan, P.D. (2001) PAST: Paleontological statistics software package for education and data analysis. *Palaeontologia Electronica*, 4, 9–18.
- Hertelendi, E., Csongor, É., Záborszky, L., Molnár, I., Gál, I., Györffy, M., Nagy, S. (1989) Counting system for high precision C-14 dating. *Radiocarbon*, 31(3), 399–406.
- Hertelendi, E., Kalicz, N., Raczky, P., Horváth, F., Veres, M., Svingor, É., Futó, I., Bartosiewicz, L. (1995) Re-evaluation of the Neolithic in eastern Hungary based on calibrated radiocarbon dates. *Radiocarbon*, 37(2), 239–244.
- Hua, Q., Turnbull, J.C., Santos, G.M., Rakowski, A.Z., Ancapichún, S., De Pol-Holz, R., Hammer, S., Lehman, S.J., Levin, I., Miller, J.B., Palmer, J.G., Turney, C.S.M. (2021) Atmospheric radiocarbon for the period 1950–2019. *Radiocarbon*, 64(4), 723–745.
- Janovics, R., Futó, I., Molnár, M. (2018) Sealed tube combustion method with MnO₂ for AMS ¹⁴C measurement. *Radiocarbon*, 60(5), 1347–1355.
- Joosten, H., Clarke, D. (2002) *Wise Use of Mires and Peatlands*. International Mire Conservation Group and International Peat Society, Jyväskylä, Finland, 304 pp.
- Kabała, C., Charzyński, P., Chodorowski, J., Drewnik, M., Glina, B., Greinert, A., Hulisz, P., Jankowski, M., Jonczak, J., Łabaz, B., Łachacz, A., Marzec, M., Mendyk, Ł., Musiał, P., Musielok, Ł., Smreczak, B., Sowiński, P., Świtoniak, M., Uzarowicz, Ł., Waroszewski, J. (2019) Polish soil classification, 6th edition - principles, classification scheme and correlations. *Soil Science Annual*, 70(2), 71–97.
- Kobashi, T., Severinghaus, J., Brook, E., Barola, J.-M., Grachev, A. (2007) Precise timing and characterization of abrupt climate change 8200 years ago from air trapped in polar ice. *Quaternary Science Reviews*, 26, 1212–1222.
- Łachacz, A., Nitkiewicz, S. (2021) Classification of soils developed from bottom lake deposits in north-eastern Poland. *Soil Science Annual*, 72(2), 140643, 14 pp.
- Li, C.H., Li, Y.X., Zheng, Y.F., Yu, S.Y., Tang, L.Y., Li, B.B., Cui, Q.Y. (2018) A high-resolution pollen record from East China reveals large climate variability near the Northgrippian-Meghalayan boundary (around 4200 years ago) exerted societal influence. *Palaeogeography, Palaeoclimatology, Palaeoecology*, 512, 156–165.
- Magiera, T., Szuszkiewicz, M., Michczyński, A., Chróst, L., Szuszkiewicz, M. (2021) Peat bogs as archives of local ore mining and smelting activities over the centuries: A case study of Miasteczko Śląskie (Upper Silesia, Poland). *CATENA*, 198, 105063, 13 pp.
- Mărculeţ, C., Mărculeţ, I. (2016) Condiții climatice favorabile și restrictive pentru cultura plantelor în depresiunea Alba Iulia - Turda (Favourable and restrictive climatic conditions for plant culture in



- the Alba Iulia - Turda depression). *Pangeea*, 16, 55–69 (in Romanian).
- Molnár, M., Janovics, R., Major, I., Orsovski, J., Gönczi, R., Veres, M., Leonard, A.G., Castle, S.M., Lange, T.E., Wacker, L., Hajdas, I., Jull, A.J.T. (2013a) Status report of the new AMS ¹⁴C sample preparation lab of the Hertelendi laboratory of environmental studies (Debrecen, Hungary). *Radiocarbon*, 55(2), 665–676.
- Molnár, M., Rinyu, L., Veres, M., Seiler, M., Wacker, L., Sýnal, H.-A. (2013b) EnvironMICADAS: A mini ¹⁴C AMS with enhanced gas ion source interface in the Hertelendi Laboratory of Environmental Studies (HEKAL), Hungary. *Radiocarbon*, 55(2–3), 338–344.
- Munsell Color Company (1954) Munsell Soil Color Charts. Munsell Color Company Inc., Baltimore MD, USA.
- Oldfield, F., Thompson, R., Barber, K.E. (1978) Changing atmospheric fallout of magnetic particles recorded in recent ombrotrophic peat sections. *Science*, 199, 679–680.
- Pop, E. (1932) Contribuții la istoria vegetației cuaternare din Transilvania (Contributions to the history of Quaternary vegetation in Transylvania). *Buletinul Grădinii Botanice și Muzeului Botanic Cluj (Bulletin of the Cluj Botanical Garden and Museum)*, 12, 29–102 (in Romanian).
- Pop, E. (1960) *Mlaștinile de turba din Republica Populară Română (The Peat Bogs of the People's Republic of Romania)*. Editura Academiei Republicii Populare Române (Publishing House of the Academy of the Romanian People's Republic), Bucharest, 511 pp. (in Romanian).
- Reimer, P., Austin W., Bard E., Bayliss A. and 38 others (2020) The IntCal20 Northern Hemisphere Radiocarbon Age Calibration Curve (0–55 cal kBP). *Radiocarbon*, 62(4), 725–757.
- Rinyu, L., Orsovski, G., Futó, I., Veres, M., Molnár, M. (2015) Application of zinc sealed tube graphitization on sub-milligram samples using EnvironMICADAS. *Nuclear Instruments and Methods in Physics Research Section B: Beam Interactions with Materials and Atoms*, 361, 406–413.
- Roland, T.P., Caseldine, C.J., Charman, D.J., Turney, C.S.M., Amesbury, M.J. (2014) Was there a 4.2 ka event in Great Britain and Ireland? Evidence from the peatland record. *Quaternary Science Reviews*, 83, 11–27.
- Rydin, H., Jeglum, J.K. (2006) *The Biology of Peatlands*. First edition, Oxford University Press, Oxford, UK, 354 pp.
- Sandgren, P., Snowball, I. (2002) Application of mineral magnetic techniques to paleolimnology. In: Last, W.M., Smol, J.P. (eds.) *Tracking Environmental Change Using Lake Sediments. Developments in Paleoenvironmental Research Vol. 2*, Springer, Dordrecht, 217–237.
- Shotyk, W. (1988) Review of the inorganic geochemistry of peats and peatland waters. *Earth-Science Reviews*, 25, 95–176.
- Staubwasser, M., Sirocko, F., Grootes, P.M., Segl, M. (2003) Climate change at the 4.2 ka BP termination of the Indus valley civilization and Holocene south Asian monsoon variability. *Geophysical Research Letters*, 30(8), 1425, 4 pp.
- Stefanescu, M., Dicea, O., Butac, A., Ciulavu, D. (2006) Hydrocarbon ecology of the Romanian Carpathians, their foreland, and the Transylvanian Basin. In: Golonka, J., Picha, F.J. (eds.) *The Carpathians and their Foreland: Geology and Hydrocarbon Resources*, AAPG Memoir 84, American Association of Petroleum Geologists (AAPG), Tulsa OK, USA, 419–421.
- Sümeği, P.A. (2001) *A negyedidőszak földtanának és öskörnyezettanának alapjai (Foundations of Quaternary Geology and Palaeoenvironment)*. JATEPress, Szeged, 224 pp. (in Hungarian).
- Sümeği, P., Magyari, E., Dániel, P., Hertelendi, E., Rudner, E. (1999) A kardoskúti Fehér-tó negyedidőszaki fejlődéstörténetének rekonstrukciója (Reconstruction of the Quaternary development history of Lake Fehér in Kardoskút). *Földtani Közlöny*, 129, 479–519 (in Hungarian).
- Sümeği, P., Náfrádi, K., Molnár, D., Sávai, Sz. (2015) Results of paleoecological studies in the loess region of Szeged-Óthalom (SE Hungary). *Quaternary International*, 372, 66–78.
- Sýnal, H.A., Stocker, M., Suter, M. (2007) MICADAS: A new compact radiocarbon AMS system. *Nuclear Instruments and Methods in Physics Research Section B: Beam Interactions with Materials and Atoms*, 259(1), 7–13.
- Tanțău, I., Reille, M., de Beaulieu, J.L., Fărcaș, S., Brewer, S. (2009) Holocene vegetation history in Romanian Subcarpathians. *Quaternary Research*, 72(2), 164–173.
- Tanțău, I., Feurdean, A., De Beaulieu, J.L., Reille, M., Fărcaș, S. (2014) Vegetation sensitivity to climate changes and human impact in the Harghita Mountains (Eastern Romanian Carpathians) over the past 15,000 years. *Journal of Quaternary Science*, 29(2), 141–152.
- Tapody, R.O., Gulyás, S., Töröcsik, T., Sümeği, P., Molnár, D., Sümeği, B.P., Molnár, M. (2018) Radiocarbon-dated peat development: Anthropogenic and climatic signals in a Holocene raised bog and lake profile from the eastern part of the Carpathian Basin. *Radiocarbon*, 60(4), 1215–1226.



- Tapody, R.O., Sümegi, P., Molnár, D., Karlik, M., Töröcsik, T., Cseh, P., Makó, L. (2021) Sedimentological-geochemical data based reconstruction of climate changes and human impacts from the peat sequence of Round Lake in the western foothill area of the Eastern Carpathians, Romania. *Quaternary*, 4, 18, 29 pp.
- Troels-Smith, J. (1955) *Karakterisering af løse jordarter (Characterisation of Unconsolidated Sediments)*. Danmarks Geologiske Undersøgelse 3(10), Reitzels Forlag, Copenhagen, 101 pp. (in Danish).
- Vári, T.Zs. (2021) *Egy tőzegmohaláp fejlődéstörténete (The Evolutionary History of a Sphagnum Peat Bog)*. MSc thesis, University of Szeged, Szeged, 23–24 (in Hungarian). Online at: <https://diploma.bibl.u-szeged.hu/id/eprint/124060/>, accessed 06 Apr 2024.
- Vári, T.Zs., Molnár, D., Sümegi, P., Sümegi, B.P., Töröcsik, T., Szakál, E., Benyó-Korcsmáros, R. (2020a) Holocene environmental history of the Bottomless Lake (Tăul fără fund) *Sphagnum* peat bog in Băgău, Romania. *Studia Quaternaria*, 37(2), 69–77.
- Vári, T.Zs., Sümegi, P., Sümegi, B.P., Töröcsik, T., Tapody, R.O., Molnár, D., Benyó-Korcsmáros, R. (2020b) A magyarbágói Feneketlen-tavi tőzegmohaláp negyedidőszak végi környezettörténete (The late Quaternary environmental history of the Bottomless Lake peat bog in Băgău). In: Töröcsik, T., Gulyás, S., Molnár, D., Náfrádi, K. (eds.) *Környezettörténet. Tanulmányok Sümegi Pál professzor 60 éves születésnapjára (Environmental History. Studies for the 60th Birthday Greeting of Professor Pál Sümegi)*, Geolitera, Szeged, 549–560 (in Hungarian).
- Vári, T.Zs., Gulyás, S., Sümegi, P. (2023) Reconstructing the paleoenvironmental evolution of Lake Kolon (Hungary) through integrated geochemical and sedimentological analyses of Quaternary sediments. *Quaternary*, 6(3), 39, 20 pp.
- Wacker, L., Christl, M., Synal, H.A. (2010) Bats: A new tool for AMS data reduction, *Nuclear Nuclear Instruments and Methods in Physics Research Section B: Beam Interactions with Materials and Atoms*, 268(7–8), 976–979.

Submitted 31 Aug 2023, revision 02 Apr 2024
Editor: Olivia Bragg

Author for correspondence: Tamás Zsolt Vári, Department of Geology and Palaeontology, University of Szeged, Egyetem Street 2–6, Szeged, H–6722, Hungary. E-mail: varitamaszsolt@gmail.com